

DECEMBER 27 2024

Role of air sinuses in sound reception of the Yangtze finless porpoise: A numerical study

Wenzhan Ou ; Zhongchang Song ; Xin Ye; Chuang Zhang; Ding Wang; Kexiong Wang; Yu Zhang 

 Check for updates

J. Acoust. Soc. Am. 156, 4279–4288 (2024)

<https://doi.org/10.1121/10.0034747>



Articles You May Be Interested In

Numerical study of biosonar beam forming in finless porpoise (*Neophocaena asiaeorientalis*)

J. Acoust. Soc. Am. (October 2014)

The ontogeny of echolocation in a Yangtze finless porpoise (*Neophocaena phocaenoides asiaeorientalis*)

J. Acoust. Soc. Am. (August 2007)

Noise-induced temporary threshold shift and recovery in Yangtze finless porpoises *Neophocaena phocaenoides asiaeorientalis*

J. Acoust. Soc. Am. (July 2011)



ASA

Advance your science and career as a member of the **Acoustical Society of America**

[LEARN MORE](#)

Role of air sinuses in sound reception of the Yangtze finless porpoise: A numerical study

Wenzhan Ou,^{1,2} Zhongchang Song,^{1,2,a)} Xin Ye,^{1,2} Chuang Zhang,^{1,2} Ding Wang,³ Kexiong Wang,³ and Yu Zhang^{1,2,b)}

¹Key Laboratory of Underwater Acoustic Communication and Marine Information Technology of the Ministry of Education, College of Ocean and Earth Sciences, Xiamen University, Xiamen 361005, China

²State Key Laboratory of Marine Environmental Science, College of Ocean and Earth Sciences, Xiamen University, Xiamen 361005, China

³Institute of Hydrobiology, Chinese Academy of Sciences, Wuhan 430072, China

ABSTRACT:

Although air sinuses are prevalent in odontocetes and are an integral component of their sound reception system, the acoustic function of these air-filled structures remains largely unknown. To address this, we developed a numerical model using computed tomography data from a Yangtze finless porpoise (*Neophocaena asiaorientalis asiaorientalis*) to investigate the role of the air sinuses in sound reception. By comparing sound reception characteristics between model cases with and without the air sinuses, we found that the air sinuses improved sound reception directivity. Across frequencies from 1 to 100 kHz, the directivity indexes for cases with and without the air sinuses ranged from 0.35 to 5.64 dB and 0.23 to 4.12 dB, respectively. Additionally, the air sinuses increased amplitude differences in received sounds, with maximum values of 2.05, 2.78, and -2.38 dB for the front-to-behind, ipsilateral-to-contralateral, and top-to-bottom aspects, respectively. These results indicate that the air sinuses effectively provided acoustic isolation for the bony ear complexes from the behind, contralateral, and top aspects, thereby enhancing asymmetric sound reception dominated by the front, ipsilateral, and bottom aspects. This study contributes to a deeper understanding of odontocete sound reception and sheds light on the significant role of the air sinuses in this context. © 2024 Acoustical Society of America. <https://doi.org/10.1121/10.0034747>

(Received 22 June 2024; revised 30 October 2024; accepted 3 December 2024; published online 27 December 2024)

[Editor: Klaus Lucke]

Pages: 4279–4288

I. INTRODUCTION

Odontocetes, including porpoises, dolphins, and toothed whales, have evolved a superior biosonar system to facilitate their survival in aquatic environments (Au, 1993; Au and Hastings, 2008). The biosonar system is a highly sophisticated multiphase medium consisting of solid, soft, and air-filled structures (Norris, 1980; Rauschmann *et al.*, 2006; Cranford *et al.*, 1996; Cranford *et al.*, 2008a; Cranford *et al.*, 2008b). It demonstrates excellent echolocation performance even under highly noisy and reverberant conditions (Au and Snyder, 1980; Au, 1993; Martin *et al.*, 2005), which is partly attributed to well-developed sound transmission and reception subsystems (Au and Moore, 1984; Au *et al.*, 1986; Aroyan, 2001; Zhang *et al.*, 2017). Researchers have dedicated efforts to understanding the mechanism of both subsystems. However, studies on the sound transmission system have outpaced those on the sound reception system.

In contrast to terrestrial mammals, odontocetes lack pinnae and their external auditory canals are considered vestigial (Ketten, 1992, 1997; Nummela *et al.*, 2007). These marine mammals have developed specific functional structures to replace the pinnae and external auditory canals,

enabling underwater sound reception. Their sound reception involves a suite of anatomical structures including air sinuses, mandibular fats, mandible, and bony ear complexes (Cranford *et al.*, 2008a; Cranford *et al.*, 2008b; Cranford *et al.*, 2010). Increasing evidence suggests that these structures form various sound reception pathways, sending sounds from water to the bony ear complexes (Norris, 1964, 1968; Cranford *et al.*, 2008a; Song *et al.*, 2018). A widely accepted pathway is the “jaw hearing” pathway proposed by Norris, where sounds entering from the external mandibular fats traverse the posterior portion of the mandible, known as the pan bone, and eventually travel along the internal mandibular fats to the bony ear complexes (Norris, 1964, 1968). This concept has garnered support from a wealth of behavioral, psychoacoustic, and numerical studies (Brill *et al.*, 1988; Au *et al.*, 1998; Møhl *et al.*, 1999; Aroyan, 2001; Cranford *et al.*, 2008a; Song *et al.*, 2018). Over the last two decades, researchers have proposed additional hypotheses to explain odontocete sound reception, revealing different pathways. Using a numerical model of Cuvier’s beaked whales, Cranford *et al.* (2008a) found a “gular pathway” where sounds enter the internal mandibular fats from the medial portion of the mandible wall and reach the bony ear complexes. Later on, Song *et al.* (2018) emphasized the importance of the mandibular tip as an ingress for sounds

^{a)}Email: songzhongchang@foxmail.com

^{b)}Email: yuzhang@xmu.edu.cn

into the sound reception system and proposed a “mandible-fat” pathway based on the numerical simulations of finless porpoises. This pathway suggests that sounds propagate along the solid mandible and internal mandibular fats to reach the bony ear complexes, potentially explaining the high sensitivity of Beluga whales, Yangtze finless porpoises, and Risso’s dolphins to acoustic stimulus at their rostrum tip (Mooney *et al.*, 2008; Mooney *et al.*, 2014; Mooney *et al.*, 2015). Sound reception in odontocetes is complex and these distinct pathways likely function at different directions and frequencies, allowing for the simultaneous collection of acoustic information from wide spatial and frequency scales (Popov *et al.*, 2016).

Sound propagation in these pathways relies on specific anatomical structures. The external mandibular fats guide sound into the sound reception system from water through acoustic impedance matching, playing an important role in the “jaw hearing” pathway (Norris, 1964, 1968; Varanasi *et al.*, 1975; Wei *et al.*, 2015). The internal mandibular fats function as a low-speed waveguide to direct sounds toward the bony ear complexes (Brekhovskikh *et al.*, 2003; Song *et al.*, 2021a; Ou *et al.*, 2023). These mandibular fats also increase the amplitude of sounds received from the front to some extent (Aroyan, 2001; Song *et al.*, 2023). Additionally, the mandible serves to send sounds toward the bony ear complexes via bone conduction, which is

particularly significant in the “mandible-fat” pathway (Song *et al.*, 2018). Recent studies suggest that reverberating sounds within the solid mandible improve the accuracy of source localization (Reinwald *et al.*, 2018; Nooghabi *et al.*, 2021). While many studies have explored the acoustic function of the mandible, mandibular fat bodies, and bony ear complexes, the air sinuses have received scant attention.

The air sinuses occupy a significant volume in the lower head region of odontocetes (Houser *et al.*, 2004; Cranford *et al.*, 2008b). These paired, air-filled structures primarily comprise pterygoid and peribullary sinuses, surrounding the superior, medial, and dorsal aspects of the bony ear complexes (Aroyan, 2001; Rauschmann *et al.*, 2006; Reidenberg and Laitman, 2008). The air sinuses can provide sufficient volume to fill the tympanic cavity, facilitating the efficient operation of the ossicular chain (Fraser and Purves, 1960; Nummela *et al.*, 1999a; Nummela *et al.*, 1999b; Hemilä *et al.*, 2001). It is speculated that high hydrostatic pressure compresses these sinuses and compromises sound reception. If so, the volume of these sinuses potentially determines the maximum dive depth of odontocetes (Cranford *et al.*, 2008b). Previous research suggests that the air sinuses improve the forward sound reception directivity of common dolphins (Aroyan, 2001). Additionally, the air sinuses may serve as acoustic shields, insulating the bony ear complexes from noises such as the echolocation clicks generated by the

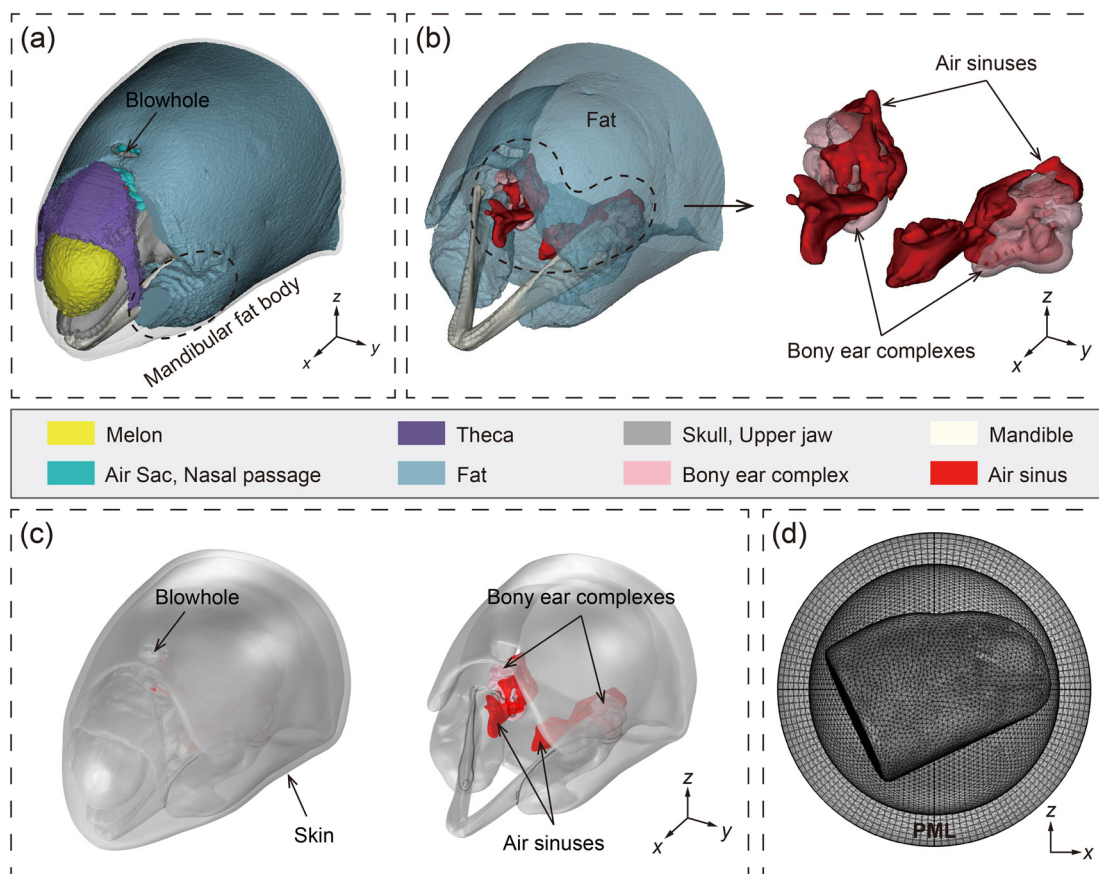


FIG. 1. (Color online) (a) Biosonar and (b) sound reception system of the finless porpoise. (c) Biosonar model. (d) Numerical model, where PML represents the perfectly matched layer.

forehead (Houser *et al.*, 2004). Air-filled structures are integral to both the sound transmission and reception systems of odontocetes. It is well-established that in the sound transmission system, air-filled structures including nasal passage and air sacs can reflect sounds emitted by the phonic lips to form forward directional beams (Wei *et al.*, 2016; Wei *et al.*, 2018; Song *et al.*, 2017). However, the role of the air sinuses in sound reception remains largely unknown.

In this study, we aimed to probe into the potential role of the air sinuses in odontocete sound reception. To achieve this objective, we used computed tomography (CT) scanning to reconstruct the biosonar structures of a Yangtze finless porpoise (*Neophocaena asiaeorientalis asiaeorientalis*) and further developed a three-dimensional numerical model. This model was employed to explore the sound reception of this species and assess the impact of the air sinuses.

II. MATERIALS AND METHODS

A. CT scan and reconstruction

The animal subject of this study was a stranded and deceased Yangtze finless porpoise. The day after its demise, it underwent a CT scan at the Department of Radiology, Zhongshan Hospital, Wuhan University (Wuhan, China). A dual-source CT scanner, SOMATOM Definition (Munich, Germany), was used for the scan with a resolution of 1 mm at a power setting of 120 kV × 76 mA. The resulting CT images were processed to reconstruct the biosonar structures of the finless porpoise [Fig. 1(a)]. The sound transmission system in the forehead primarily consisted of the melon, theca (dense connective tissue), upper jaw, skull, nasal passage, and air sacs. The sound reception system in the lower head included the air sinuses, mandibular fats, mandible, and bony ear complexes [Fig. 1(b)]. The mandibular fats were distributed both inside and outside the mandible. The air sinuses surrounded the superior, medial, and dorsal aspects of the bony ear complexes and extended anteriorly. The biosonar structures of this species closely resembled those of other odontocetes (Cranford *et al.*, 2008b; Cranford *et al.*, 2010; Song *et al.*, 2018).

B. Numerical modeling

The reconstructed structures were used to develop a three-dimensional biosonar model [Fig. 1(c)]. The biosonar model was placed in a spherical computational domain with a radius of 0.15 m, of which the outermost layer was set as the perfectly matched layer to eliminate reflection at the domain boundary, simulating an open infinite domain [Fig. 1(d)]. The numerical model accounted for acoustic-structure coupling, treating bony structures as solid media and the others as fluid media. The bony structures were assigned a density of 2035 kg/m³, with longitudinal and shear wave speeds of 3380 and 2200 m/s, respectively (Graf *et al.*, 2008; Song *et al.*, 2021b). The density and longitudinal wave speed for the theca and fatty structures were set as 1070 kg/m³ and 1720 m/s, and 940 kg/m³ and 1380 m/s, respectively (Wei *et al.*, 2015; Song *et al.*, 2023). For the air-filled structures, these values were 1.21 kg/m³ and 343 m/s. The domain outside the biosonar model was filled with water, with a density of 998 kg/m³ and a sound speed of 1483 m/s. To examine the impact of the air sinuses, we established two model cases: (1) the “water-filled” case, in which the air sinuses were replaced by water and (2) the “air-filled” case, in which the air sinuses were still filled with air.

A background pressure field emitted plane waves with various incidence directions and a reference amplitude of 1 Pa. The incidence direction (θ, φ) was defined by the elevation angle θ and azimuth angle φ [Fig. 2(a)]. The elevation and azimuth angles ranged from -90° to 90° and -180° to 180° , respectively, with a step of 6° . The perfectly matched layer was divided into hexahedral elements and the remaining computational domain was divided into tetrahedral elements, ensuring that the maximum element size was less than one-fifth of the wavelength. The three-dimensional simulations of the numerical model were performed using COMSOL MULTIPHYSICS software (Stockholm, Sweden). Following calculations, the sound pressure at the surface of the tympanic bulla was averaged to determine the received amplitude. These received amplitudes from all the incidence directions were mapped onto a global projection to fully visualize the sound reception directivity pattern [Fig. 2(b)].

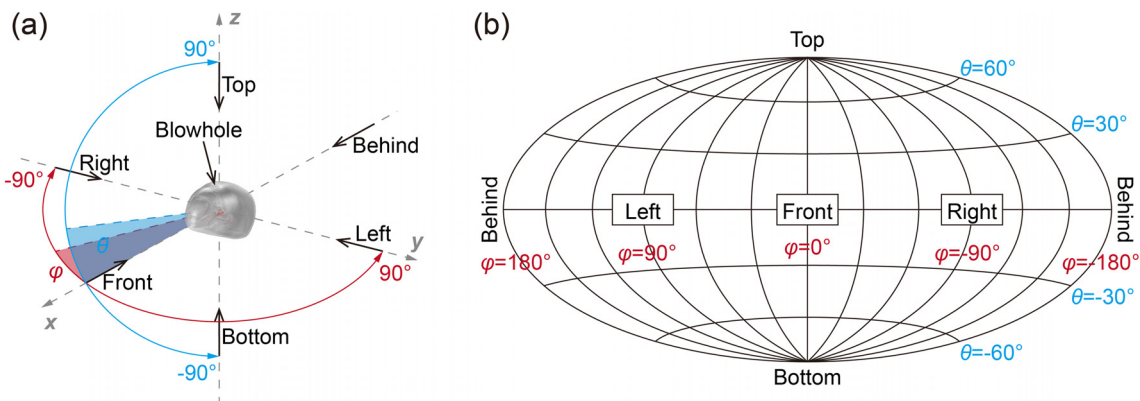


FIG. 2. (Color online) (a) Schematic diagram of the incidence direction of plane waves. (b) Global projection.

The directivity index (DI) describes the directivity of a directional receiver compared to that of an omnidirectional receiver and is expressed as (Accomando *et al.*, 2020; Au and Moore, 1984)

$$DI = 10 \log_{10} \left[\frac{4\pi}{\int_{-\pi}^{\pi} \int_{-\pi/2}^{\pi/2} b(\theta, \varphi) \cos \theta d\theta d\varphi} \right], \quad (1)$$

where $b(\theta, \varphi)$ is the beam pattern. The DI was used to evaluate the sound reception directivity of the finless porpoise. However, the DI did not capture the asymmetry of the directivity pattern. Therefore, we introduced three additional parameters to quantify sound reception asymmetry from three axial directions. The first parameter is the front-to-behind ratio (FBR), defined as the ratio of the power received from the front to that received from the behind, calculated using the formula

$$FBR = 10 \log_{10} \left[\frac{\int_{-\pi/2}^{\pi/2} \int_{-\pi/2}^{\pi/2} b(\theta, \varphi) \cos \theta d\theta d\varphi}{\int_{-\pi}^{-\pi/2} \int_{-\pi/2}^{\pi/2} b(\theta, \varphi) \cos \theta d\theta d\varphi + \int_{\pi/2}^{\pi} \int_{-\pi/2}^{\pi/2} b(\theta, \varphi) \cos \theta d\theta d\varphi} \right]. \quad (2)$$

The second parameter, the ipsilateral-to-contralateral ratio (ICR), quantifies the ratio of the power received from the ipsilateral side to that received from the contralateral side and is expressed as

$$ICR = 10 \log_{10} \left[\frac{\int_0^{\pi} \int_{-\pi/2}^{\pi/2} b(\theta, \varphi) \cos \theta d\theta d\varphi}{\int_{-\pi}^0 \int_{-\pi/2}^{\pi/2} b(\theta, \varphi) \cos \theta d\theta d\varphi} \right], \quad (3)$$

$$ICR = 10 \log_{10} \left[\frac{\int_{-\pi}^0 \int_{-\pi/2}^{\pi/2} b(\theta, \varphi) \cos \theta d\theta d\varphi}{\int_0^{\pi} \int_{-\pi/2}^{\pi/2} b(\theta, \varphi) \cos \theta d\theta d\varphi} \right], \quad (4)$$

where Eqs. (3) and (4) are applied to the left and right ears, respectively. The third parameter, the top-to-bottom ratio (TBR), quantifies the ratio of the power received from the top to that received from the bottom and is expressed as

$$TBR = 10 \log_{10} \left[\frac{\int_{-\pi}^{\pi} \int_0^{\pi/2} b(\theta, \varphi) \cos \theta d\theta d\varphi}{\int_{-\pi}^{\pi} \int_{-\pi/2}^0 b(\theta, \varphi) \cos \theta d\theta d\varphi} \right]. \quad (5)$$

III. RESULTS

Sound pressure fields were analyzed for forward incidence at 2, 8, 30, 50, and 90 kHz (Fig. 3). It was observed that the mandibular fats played a significant role in amplifying incident sounds and directing them towards the bony ear complexes. The dense skull effectively blocked incident sounds at its front, resulting in a region of low amplitude

behind it. Comparison between the two cases indicates that the air sinuses attenuated the amplitude of the surrounding acoustic field, with this attenuation being more pronounced at lower frequencies.

The received amplitudes from the forward incidence were analyzed across the frequency range from 1 to 100 kHz (Fig. 4). In both cases, higher received amplitudes were observed at high frequencies compared to low frequencies. In the “air-filled” case, significant attenuation in received amplitudes was noted below 30 kHz. The “air-filled” case exhibited lower received amplitudes than the “water-filled” case across the frequency range. The differences in received amplitudes between the two cases were more pronounced at low frequencies than at high frequencies.

The sound pressure fields of the air sinuses and bony ear complexes were examined at 50 kHz with various incidence directions (Fig. 5). In the “water-filled” case, the surface of the air sinuses showed complex and non-zero sound pressure distributions [Fig. 5(a)]. The amplitudes received by the bony ear complexes did not reveal discernible regularities in response to sounds incident from different directions. In contrast, the surface sound pressures of the air sinuses consistently remained zero in the “air-filled” case [Fig. 5(b)]. The bony ear complexes received sounds with an amplitude of 8.61 dB higher from the front than from behind. For laterally originating sounds, the received amplitude was 4.72 dB greater from the ipsilateral aspect than the contralateral aspect. Vertically, the bony ear complexes exhibited a higher amplitude for sounds coming from the bottom than the top, with a difference of 7.43 dB.

Monaural directivity patterns were analyzed at 2, 8, 30, 50, and 90 kHz (Fig. 6). Overall, the “water-filled” case exhibited relatively weak monaural directivity across the examined frequencies, with broad downward beams on the same side of both ears [Fig. 6(a)]. However, at 8 kHz, the directivity patterns showed complexity with unexpected

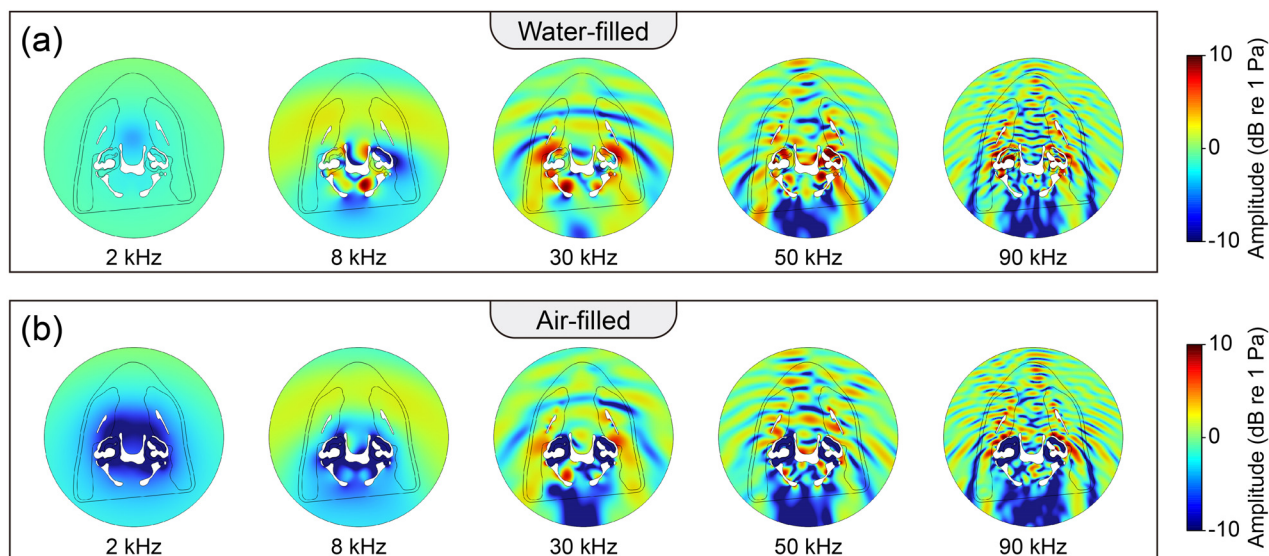


FIG. 3. (Color online) Sound pressure fields for forward incidence ($\theta = 0, \varphi = 0$) in the (a) “water-filled” case and (b) “air-filled” case. The color bars represent sound pressure amplitude where values greater than 0 dB indicate amplification and values less than 0 dB indicate attenuation of the incident sounds.

upward energy leakage in both ears. In the “air-filled” case, the presence of air sinuses effectively mitigated this upward energy leakage [Fig. 6(b)]. Shadowed regions indicating low received amplitude expanded on the contralateral top aspect of both ears. The air sinuses contributed to more focused receiving beam patterns. As the frequency increased, the orientation of the main beam shifted from the ipsilateral bottom towards the front.

Sound reception directivity in both cases was estimated using the DI (Fig. 7). The DIs displayed an increasing trend with frequency in both cases. Across the frequency range from 1 to 100 kHz, the DIs for the “water-filled” case and “air-filled” case ranged from 0.23 to 4.12 dB and 0.35 to 5.64 dB, respectively. Overall, the “air-filled” case showed higher DIs than the “water-filled” case, with greater differences at higher frequencies than lower ones.

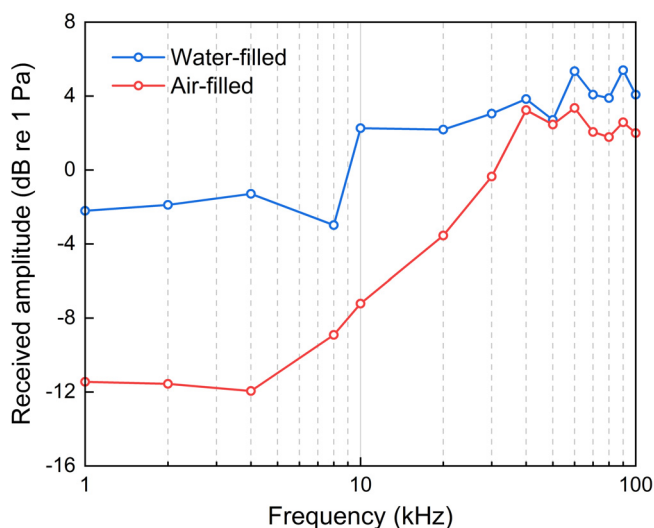


FIG. 4. (Color online) Comparison of the received amplitudes from the forward incidence in both cases.

Asymmetry in sound reception was quantified from three axial directions using the FBR, TBR, and ICR (Fig. 8). The FBRs and ICRs were higher in the “air-filled” case compared to the “water-filled” case, whereas the “air-filled” case exhibited lower TBRs than the “water-filled” case. In the “air-filled” case, the FBR, ICR, and TBR ranged from 0.04 to 2.36 dB, 0.15 to 3.99 dB, and -2.65 to 0.27 dB, respectively. The difference in the FBR, ICR, and TBR between the two cases peaked at 30, 30, and 8 kHz, with maximum values of 2.05, 2.78, and -2.38 dB, respectively. On average across the examined frequency range, these differences were 0.79, 1.61, and -0.70 dB, respectively. These comparisons indicate that sound reception was more effective from the front, ipsilateral, and bottom aspects compared to behind, contralateral, and top aspects, respectively. The presence of air sinuses enhanced sound reception from the front, ipsilateral, and bottom aspects while diminishing that from behind, contralateral, and top aspects.

IV. DISCUSSION

Acoustic impedance, defined as the product of the density and sound speed of a medium, influences acoustic reflection and refraction. From this perspective, the air sinuses can serve as excellent sound-reflective boundaries due to their significantly lower acoustic impedance compared to surrounding tissues (Cranford *et al.*, 2008b; Reidenberg and Laitman, 2008). This notion was strongly supported by our acoustic field results, where antiphase sounds reflected by the air sinuses nearly completely counteracted incident sounds, resulting in zero sound pressure on their surface (Fig. 5). Our results further demonstrated that the air sinuses effectively isolated sounds entering the bony ear complexes from behind, contralateral, and top aspects. This acoustic isolation was clearly observed in the expanded shadowed regions corresponding to contralateral and top

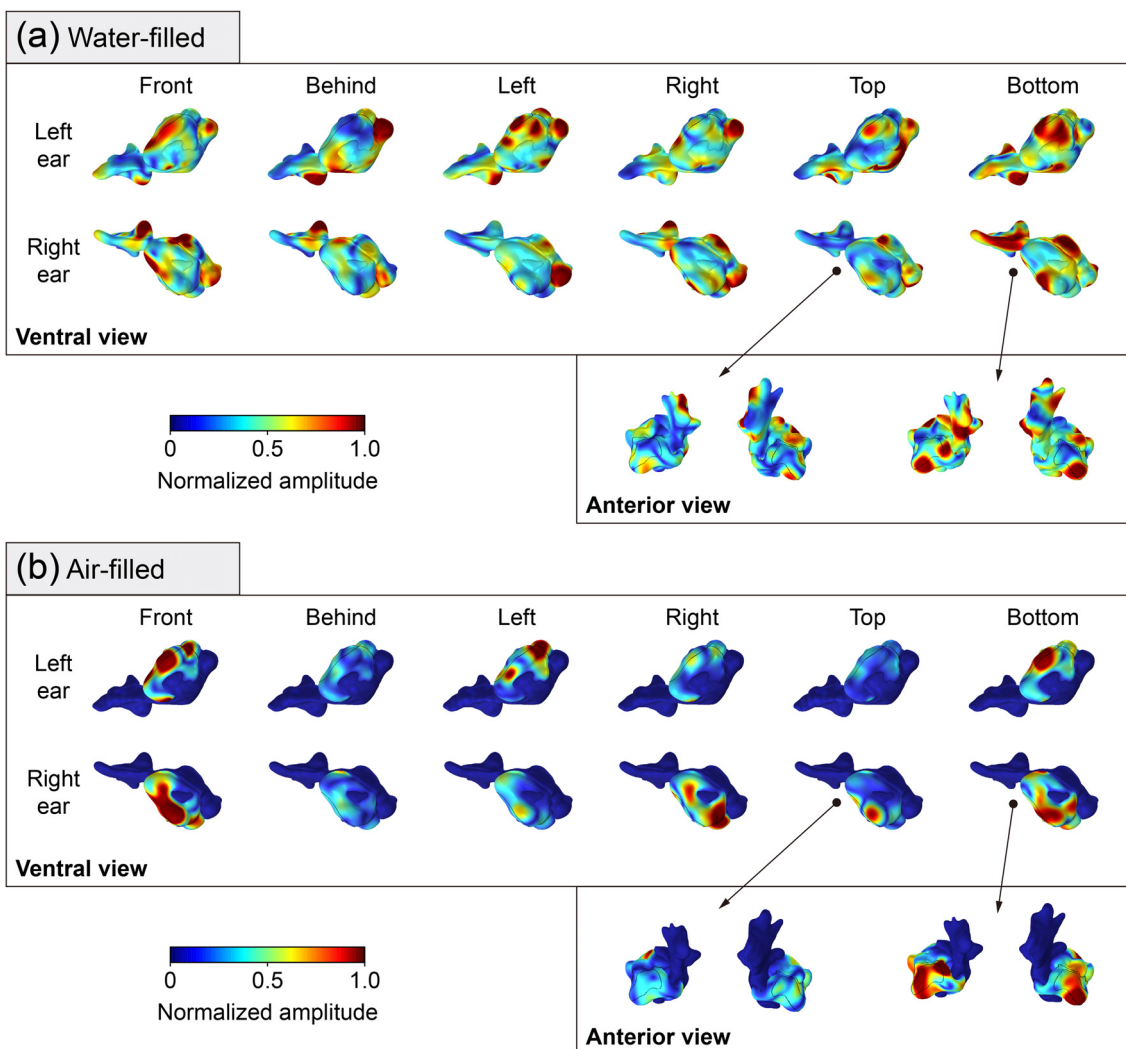


FIG. 5. (Color online) Ventral view of sound pressure fields of the air sinuses and bony ear complexes in the (a) “water-filled” case and (b) “air-filled” case, where 50 kHz sounds were incident from six distinct directions as depicted in Fig. 2. The color bars indicate normalized sound pressure amplitude.

incidences (Fig. 6), aligning with previous research (Aroyan, 2001). Additionally, the air sinuses contributed to enhancing the sound reception directivity of the finless porpoise (Fig. 7), consistent with observations in common dolphins (Aroyan, 2001). This consistency suggests a similar functional role of the air sinuses in sound reception across odontocetes. Au and Moore (1984) reported receiving DIs of bottlenose dolphins as 10.4, 15.3, and 20.6 dB at 30, 60, and 120 kHz, respectively, significantly higher than those estimated in this study. This difference is partly attributed to the different methods used for DI estimation. Au and Moore (1984) measured only half (180° range) of the directivity patterns in the horizontal and vertical planes, and estimated the DI based solely on the frontal hemispheric pattern. This may lead to an overestimation compared to a full-spheric DI estimation. Moreover, bottlenose dolphins exhibit higher DIs than harbor porpoises despite using similar estimation methods (Kastelein *et al.*, 2005; Popov *et al.*, 2006; Accomando *et al.*, 2020). This suggests that size and anatomical variations in the sound reception systems among

odontocetes may also contribute to the observed difference. Specifically, porpoises have smaller heads and shorter mandibles than dolphins, which probably influences sound reception. Our estimated DIs for Yangtze finless porpoises follow a similar trend to those of harbor porpoises below 60 kHz; however, a notable difference emerges at higher frequencies, likely due to the absence of the inner ear in our model.

As the frequency increases, the most sensitive azimuth angle of bottlenose dolphins approaches the midline from the side (Popov *et al.*, 2006). This frequency-dependent change in the most sensitive azimuth angle is highly similar to the shift in the azimuth angle of the main beam in this study (Fig. 6). In addition, the elevation angle of the main beam shifted from the bottom to the front with increasing frequency. Significantly, the air sinuses played a role in focusing the main beam and enhancing the frequency-dependent shift of the beam angle (Fig. 6). These findings suggest that the finless porpoise better received low-frequency sounds at the lateral bottom and high-frequency

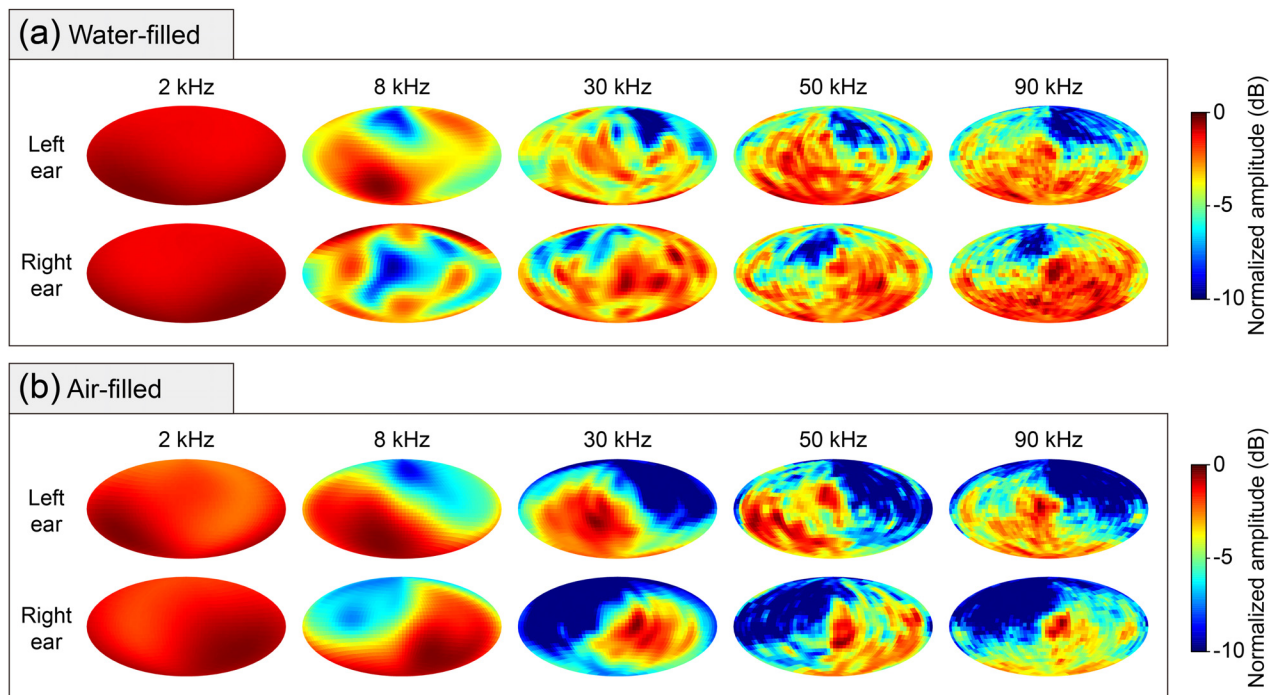


FIG. 6. (Color online) Monaural directivity patterns in the (a) “water-filled” case and (b) “air-filled” case. The color bars indicate normalized sound pressure amplitude.

sounds at the front. This conclusion is consistent with previous experimental results from the same species, which identified the meatus as the most sensitive position for low frequency (8 kHz), and the front head and the mandibular fat pad for high frequencies (54 and 120 kHz) (Mooney *et al.*, 2013). The frequency-dependent directivity shift likely resulted from different sound reception pathways operating at different frequencies and incidence directions (Popov *et al.*, 2016). The forward directivity observed at high frequencies can improve the signal-to-noise ratio of echoes, thereby facilitating biosonar echolocation (Au, 1993).

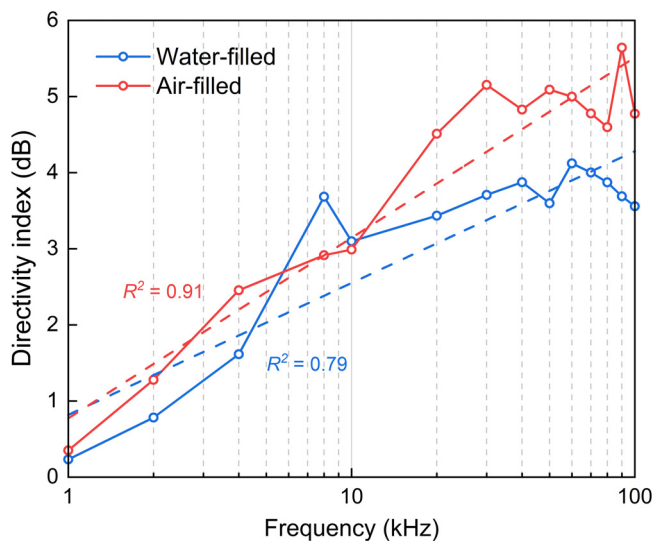


FIG. 7. (Color online) Comparison of the DIs in both cases. The dashed lines represent the trend lines.

However, the function of the lateral downward directivity at low frequencies remains unclear. For dolphins that use low-frequency whistles to communicate, frequency-dependent receiving directivity may cause the relative levels of fundamental and harmonic frequencies of whistles to vary with incidence direction, aiding in determining the whistler’s directionality (Lammers and Au, 2003). In contrast, finless porpoises do not appear to produce whistles. One possible function of the lateral directivity is to receive low-frequency cues from ambient soundscapes, facilitating self-orientation (Mooney *et al.*, 2013). Additionally, it may facilitate the passive search for soniferous prey before using active echolocation, thereby improving predation efficiency (Gannon *et al.*, 2005; Cheng *et al.*, 2023).

Our results reveal that the received amplitude from the forward incidence peaked at 50 kHz and decreased notably below this frequency (Fig. 4), which is similar to evoked potential studies indicating a V-shaped audiogram with the best sensitivity at 54 kHz in Yangtze finless porpoises (Popov *et al.*, 2005; Popov *et al.*, 2011). The presence of the air sinuses would attenuate the received amplitude by creating antiphase sounds that partly counteracted incident sounds, particularly noticeable at lower frequencies (Fig. 3). These findings suggest that the air sinuses may be an important factor in the relatively high auditory threshold observed in finless porpoises at low frequencies.

Experimental studies have indicated that odontocete sound reception exhibits asymmetry (Accomando *et al.*, 2020; Au and Moore, 1984; Kastelein *et al.*, 2005; Popov *et al.*, 2006). This study provided similar results that the finless porpoise better received sounds from the front, ipsilateral, and bottom aspects (Figs. 5 and 8). Popov *et al.* (2006)

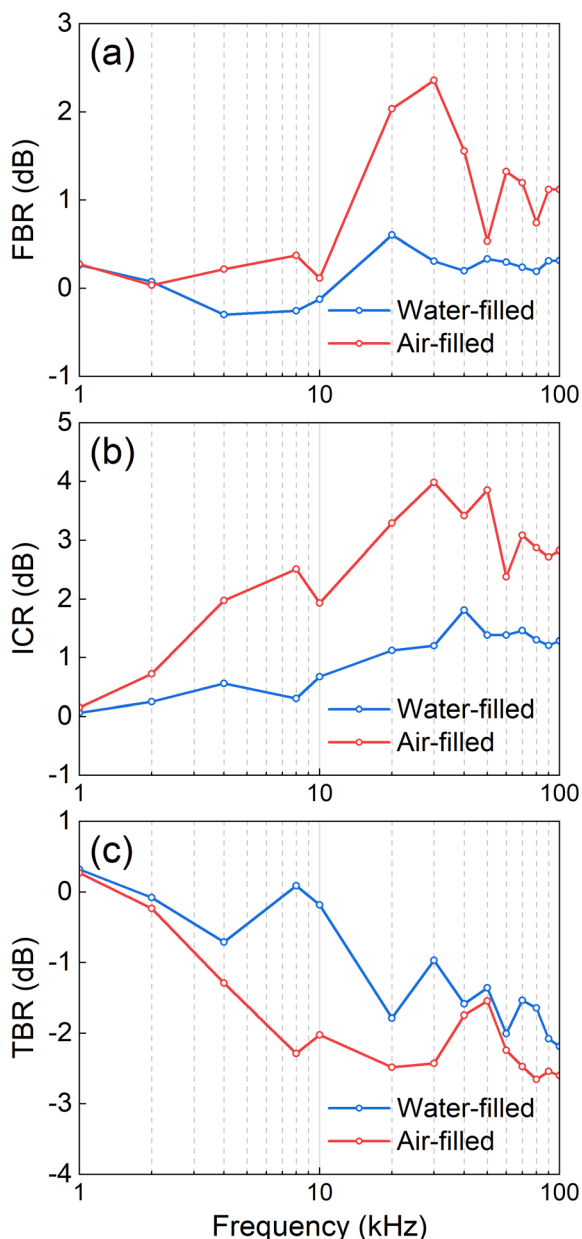


FIG. 8. (Color online) Comparison of (a) FBRs, (b) ICRs, and (c) TBRs in both cases.

found that the monaural hearing thresholds of bottlenose dolphins are consistently lower at the ipsilateral aspect than the contralateral aspect, aligning with our results [Figs. 5(b) and 8(b)]. These results demonstrate a horizontally asymmetric head-related transfer function (HRTF), which not only improves the accuracy of sound localization through significant interaural level difference (ILD) but also effectively resolves the left-right localization ambiguity resulting from the absence of binaural differences in the mid-sagittal plane (Branstetter and Mercado, 2006; Krysl and Cranford, 2016; Reinwald *et al.*, 2018; Nooghabi *et al.*, 2021). In addition, the marked amplitude difference between the top and bottom aspects underscores vertical asymmetry in the HRTF [Figs. 5(b) and 8(c)]. Similar vertical differences have been observed in other species adept at acoustically localizing

prey, such as owls and bats, which can enhance sound localization in the vertical plane (Coles and Guppy, 1988; Jen and Chen, 1988; Fuzessery, 1996; De Koning *et al.*, 2020). More importantly, our findings highlighted the significant role of the air sinuses in enhancing asymmetric sound reception (Fig. 8).

The subject of the CT scan in this study was a recently deceased specimen. Nonetheless, prior research has demonstrated the reliability of numerical modeling based on CT data from deceased specimens (Mckenna *et al.*, 2007; Cranford *et al.*, 2014; Wei *et al.*, 2023). Mckenna *et al.* (2007) reported no significant postmortem changes in the geometry, density, and sound speed of anatomical structures in bottlenose dolphins, indicating that deceased specimens can reliably approximate living specimens. However, their measurements did not include the air sinuses, which may collapse after death, potentially reducing sound reception directivity and asymmetry. Additionally, the air sinuses are pervasive in nearly all odontocetes and occupy a relatively larger volume in deep-diving species (Cranford *et al.*, 2008b; Reidenberg and Laitman, 2008). These animals may possess the ability to manipulate their air sinus volume through lung airflow controlled by the palatopharyngeal sphincter (Ridgway *et al.*, 1980; Houser *et al.*, 2004). Therefore, it is essential to further investigate whether the deformation of the air sinuses influences sound reception capability and how odontocetes adjust this capability by regulating these sinuses. One possible limitation was that this study focused only on the sound reception process from the far field to the middle ears, excluding consideration of the inner ears due to the resolution limitation of the CT scan. Future research with higher-resolution models could explore the inner ears more comprehensively, providing deeper insights into the sound reception mechanisms of odontocetes.

V. CONCLUSIONS

In this study, we developed a numerical model using CT data from a Yangtze finless porpoise to investigate the potential impact of the air sinuses on sound reception. Our findings demonstrated that these sinuses contributed to enhancing sound reception directivity. Moreover, these sinuses effectively provided acoustic isolation for the bony ear complexes from behind, contralateral, and top aspects, thereby improving sound reception asymmetry dominated from the front, ipsilateral, and bottom aspects. The enhanced sound reception directivity and asymmetry by the air sinuses have the potential to improve the effectiveness of biosonar echolocation. These results offer valuable insights into odontocete sound reception and the role of the air sinuses.

ACKNOWLEDGMENTS

This work was funded by the National Natural Science Foundation of China (Grant Nos. 12074323, 42106181, and 62231011), Major science and technology projects of Fujian Province, China (Grant No. 2021NZ033016), and the Ph.D.

Fellowship of State Key Laboratory of Marine Environmental Science at Xiamen University. We appreciate Xiaohui Xu and Zhen Xiao from the College of Ocean and Earth Sciences at Xiamen University for their valuable assistance in this research.

AUTHOR DECLARATIONS

Conflict of Interest

The authors have no conflict to disclose.

DATA AVAILABILITY

The data supporting the findings of this study are available from the corresponding author upon reasonable request.

Accomando, A. W., Mulsow, J., Branstetter, B. K., Schlundt, C. E., and Finneran, J. J. (2020). "Directional hearing sensitivity for 2–30 kHz sounds in the bottlenose dolphin (*Tursiops truncatus*)," *J. Acoust. Soc. Am.* **147**, 388–398.

Aroyan, J. L. (2001). "Three-dimensional modeling of hearing in *Delphinus delphis*," *J. Acoust. Soc. Am.* **110**, 3305–3318.

Au, W. W. L. (1993). *The Sonar of Dolphins* (Springer Science & Business Media, New York).

Au, W. W. L., and Hastings, M. C. (2008). *Principles of Marine Bioacoustics* (Springer, New York).

Au, W. W. L., Mohl, B., Nachtigall, P. E., Pawloski, J. L., and Aroyan, J. L. (1998). "Acoustic pathways of hearing in the bottlenose dolphin, *Tursiops truncatus*," *J. Acoust. Soc. Am.* **103**, 2908.

Au, W. W. L., and Moore, P. W. B. (1984). "Receiving beam patterns and directivity indices of the Atlantic bottlenose dolphin," *J. Acoust. Soc. Am.* **75**, 255–262.

Au, W. W. L., Moore, P. W. B., and Pawloski, D. (1986). "Echolocation transmitting beam of the Atlantic bottlenose dolphin," *J. Acoust. Soc. Am.* **80**, 688–691.

Au, W. W. L., and Snyder, K. J. (1980). "Long-range target detection in open waters by an echolocating Atlantic Bottlenose dolphin (*Tursiops truncatus*)," *J. Acoust. Soc. Am.* **68**, 1077–1084.

Branstetter, B. K., and Mercado, E. (2006). "Sound localization by cetaceans," *Int. J. Comp. Psychol.* **19**, 26–61.

Brekhovskikh, L. M., Lysanov, Y. P., and Lysanov, J. P. (2003). *Fundamentals of Ocean Acoustics* (Springer Science & Business Media, New York).

Brill, R. L., Sevenich, M. L., Sullivan, T. J., Sustman, J. D., and Witt, R. E. (1988). "Behavioral evidence for hearing through the lower jaw by an echolocating dolphin (*Tursiops truncatus*)," *Mar. Mammal Sci.* **4**, 223–230.

Cheng, Z., Li, Y., Pine, M. K., Zuo, T., Niu, M., and Wang, J. (2023). "Association between porpoise presence and fish choruses: Implications for feeding strategies and ecosystem-based conservation of the East Asian finless porpoise," *Integr. Zool.* **18**, 169–182.

Coles, R. B., and Guppy, A. (1988). "Directional hearing in the barn owl (*Tyto alba*)," *J. Comp. Physiol.* **163**, 117–133.

Cranford, T. W., Amundin, M., and Norris, K. S. (1996). "Functional morphology and homology in the odontocete nasal complex: Implications for sound generation," *J. Morphol.* **228**, 223–285.

Cranford, T. W., Krysl, P., and Amundin, M. (2010). "A new acoustic portal into the odontocete ear and vibrational analysis of the tympanoperiotic complex," *PLoS One* **5**, e11927.

Cranford, T. W., Krysl, P., and Hildebrand, J. A. (2008a). "Acoustic pathways revealed: Simulated sound transmission and reception in Cuvier's beaked whale (*Ziphius cavirostris*)," *Bioinspir. Biomim.* **3**, 016001.

Cranford, T. W., Mckenna, M. F., Soldevilla, M. S., Wiggins, S. M., Goldbogen, J. A., Shadwick, R. E., Krysl, P., St. Leger, J. A., and Hildebrand, J. A. (2008b). "Anatomic geometry of sound transmission and reception in Cuvier's beaked whale (*Ziphius cavirostris*)," *Anat. Rec. Adv. Integr. Anat. Evol. Biol.* **291**, 353–378.

Cranford, T. W., Trijoulet, V., Smith, C. R., and Krysl, P. (2014). "Validation of a vibroacoustic finite element model using bottlenose dolphin simulations: The dolphin biosonar beam is focused in stages," *Bioacoustics* **23**, 161–194.

De Koning, M., Beatini, J. R., Proudfoot, G. A., and Gall, M. D. (2020). "Hearing in 3D: Directional auditory sensitivity of northern saw-whet owls (*Aegolius acadicus*)," *Integr. Comp. Biol.* **60**, 1058–1067.

Fraser, F. C., and Purves, P. E. (1960). "Hearing in cetaceans: Evolution of the accessory air sacs and the structure and function of the outer and middle ear in recent cetaceans," *Bull. Br. Mus. Nat. Hist. Zool.* **7**, 1–140.

Fuzessery, Z. M. (1996). "Monaural and binaural spectral cues created by the external ears of the pallid bat," *Hear. Res.* **95**, 1–17.

Gannon, D. P., Barros, N. B., Nowacek, D. P., Read, A. J., Waples, D. M., and Wells, R. S. (2005). "Prey detection by bottlenose dolphins, *Tursiops truncatus*: An experimental test of the passive listening hypothesis," *Anim. Behav.* **69**, 709–720.

Graf, S., Megill, W. M., Blondel, P., and Clift, S. E. (2008). "Investigation into the possible role of dolphins' teeth in sound reception," *J. Acoust. Soc. Am.* **123**, 3360.

Hemilä, S., Nummela, S., and Reuter, T. (2001). "Modeling whale audiograms: Effects of bone mass on high-frequency hearing," *Hear. Res.* **151**, 221–226.

Houser, D. S., Finneran, J., Carder, D., Van Bonn, W., Smith, C., Hoh, C., Mattrey, R., and Ridgway, S. (2004). "Structural and functional imaging of bottlenose dolphin (*Tursiops truncatus*) cranial anatomy," *J. Exp. Biol.* **207**, 3657–3665.

Jen, P. H.-S., and Chen, D. (1988). "Directionality of sound pressure transformation at the pinna of echolocating bats," *Hear. Res.* **34**, 101–117.

Kastelein, R. A., Janssen, M., Verboom, W. C., and de Haan, D. (2005). "Receiving beam patterns in the horizontal plane of a harbor porpoise (*Phocoena phocoena*)," *J. Acoust. Soc. Am.* **118**, 1172–1179.

Ketten, D. R. (1992). "The marine mammal ear: Specializations for aquatic audition and echolocation," in *The Evolutionary Biology of Hearing*, edited by D. B. Webster, A. N. Popper, and R. R. Fay (Springer New York, New York), pp. 717–750.

Ketten, D. R. (1997). "Structure and function in whale ears," *Bioacoustics* **8**, 103–135.

Krysl, P., and Cranford, T. W. (2016). "Directional hearing and head-related transfer function in odontocete cetaceans," in *The Effects of Noise on Aquatic Life II*, edited by A. N. Popper and A. Hawkins (Springer, New York), pp. 583–587.

Lammers, M. O., and Au, W. W. L. (2003). "Directionality in the whistles of Hawaiian spinner dolphins (*Stenella longirostris*): A signal feature to cue direction of movement?," *Mar. Mammal Sci.* **19**, 249–264.

Martin, S. W., Phillips, M., Bauer, E. J., Moore, P. W., and Houser, D. S. (2005). "Instrumenting free-swimming dolphins echolocating in open water," *J. Acoust. Soc. Am.* **117**, 2301–2307.

Mckenna, M. F., Goldbogen, J. A., St. Leger, J., Hildebrand, J. A., and Cranford, T. W. (2007). "Evaluation of postmortem changes in tissue structure in the bottlenose dolphin (*Tursiops truncatus*)," *Anat. Rec.* **290**, 1023–1032.

Möhl, B., Au, W. W. L., Pawloski, J., and Nachtigall, P. E. (1999). "Dolphin hearing: Relative sensitivity as a function of point of application of a contact sound source in the jaw and head region," *J. Acoust. Soc. Am.* **105**, 3421–3424.

Mooney, T. A., Li, S., Ketten, D. R., Wang, K., and Wang, D. (2014). "Hearing pathways in the Yangtze finless porpoise, *Neophocaena asiaeorientalis asiaeorientalis*," *J. Exp. Biol.* **217**, 444–452.

Mooney, T. A., Nachtigall, P. E., Castellote, M., Taylor, K. A., Pacini, A. F., and Esteban, J.-A. (2008). "Hearing pathways and directional sensitivity of the beluga whale, *Delphinapterus leucas*," *J. Exp. Mar. Biol. Ecol.* **362**, 108–116.

Mooney, T. A., Yang, W.-C., Yu, H.-Y., Ketten, D. R., and Jen, I.-F. (2015). "Hearing abilities and sound reception of broadband sounds in an adult Risso's dolphin (*Grampus griseus*)," *J. Comp. Physiol. A* **201**, 751–761.

Nooghabi, A. H., Grimal, Q., Herrel, A., Reinwald, M., and Boschi, L. (2021). "Contribution of bone-reverberated waves to sound localization of dolphins: A numerical model," *Acta Acust.* **5**, 3.

Norris, K. S. (1964). "Some problems of echolocation in cetaceans," *Mar. Bioacoustics* **1**, 317–336.

- Norris, K. S. (1968). "The evolution of acoustic mechanisms in odontocete cetaceans," in *Evolution and Environment*, edited by E. T. Drake (Yale University Press, New York), pp. 297–324.
- Norris, K. S. (1980). "Peripheral sound processing in odontocetes," in *Animal Sonar Systems*, NATO Advanced Study Institutes Series, edited by R.-G. Busnel and J. F. Fish (Springer U.S., Boston), pp. 495–509.
- Nummela, S., Reuter, T., Hemilä, S., Holmberg, P., and Paukku, P. (1999a). "The anatomy of the killer whale middle ear (*Orcinus orca*)," *Hear. Res.* **133**, 61–70.
- Nummela, S., Thewissen, J. G. M., Bajpai, S., Hussain, T., and Kumar, K. (2007). "Sound transmission in archaic and modern whales: Anatomical adaptations for underwater hearing," *Anat. Rec.* **290**, 716–733.
- Nummela, S., Wägar, T., Hemilä, S., and Reuter, T. (1999b). "Scaling of the cetacean middle ear," *Hear. Res.* **133**, 71–81.
- Ou, W., Song, Z., Gao, Z., Zhang, C., Zhang, J., Hui, J., and Zhang, Y. (2023). "A porpoise-inspired receptor to enhance broadband sound reception," *Appl. Phys. Lett.* **123**, 043701.
- Popov, V. V., Supin, A. Y., Klishin, V. O., and Bulgakova, T. N. (2006). "Monaural and binaural hearing directivity in the bottlenose dolphin: Evoked-potential study," *J. Acoust. Soc. Am.* **119**, 636–644.
- Popov, V. V., Supin, A. Y., Wang, D., Wang, K., Dong, L., and Wang, S. (2011). "Noise-induced temporary threshold shift and recovery in Yangtze finless porpoises *Neophocaena phocaenoides asiaorientalis*," *J. Acoust. Soc. Am.* **130**, 574–584.
- Popov, V. V., Supin, A. Y., Wang, D., Wang, K., Xiao, J., and Li, S. (2005). "Evoked-potential audiogram of the Yangtze finless porpoise *Neophocaena phocaenoides asiaorientalis* (L)," *J. Acoust. Soc. Am.* **117**, 2728–2731.
- Popov, V. V., Sysueva, E. V., Nechaev, D. I., Lemazina, A. A., and Supin, A. Y. (2016). "Auditory sensitivity to local stimulation of the head surface in a beluga whale (*Delphinapterus leucas*)," *J. Acoust. Soc. Am.* **140**, 1218–1226.
- Rauschmann, M. A., Huggenberger, S., Kossatz, L. S., and Oelschläger, H. H. A. (2006). "Head morphology in perinatal dolphins: A window into phylogeny and ontogeny," *J. Morphol.* **267**, 1295–1315.
- Reidenberg, J. S., and Laitman, J. T. (2008). "Sisters of the sinuses: Cetacean air sacs," *Anat. Rec.* **291**, 1389–1396.
- Reinwald, M., Grimal, Q., Marchal, J., Catheline, S., and Boschi, L. (2018). "Bone-conducted sound in a dolphin's mandible: Experimental investigation of elastic waves mediating information on sound source position," *J. Acoust. Soc. Am.* **144**, 2213–2224.
- Ridgway, S. H., Carder, D. A., Green, R. F., Gaunt, A. S., Gaunt, S. L. L., and Evans, W. E. (1980). "Electromyographic and pressure events in the nasolaryngeal system of dolphins during sound production," in *Animal Sonar Systems*, edited by R.-G. Busnel and J. F. Fish (Springer U.S., Boston), pp. 239–249.
- Song, Z., Ou, W., Li, J., Zhang, C., Fu, W., Xiang, W., Wang, D., Wang, K., and Zhang, Y. (2023). "Sound reception in the Yangtze finless porpoise and its extension to a biomimetic receptor," *Biomimetics* **8**, 366.
- Song, Z., Zhang, C., Zhang, J., Ou, W., and Zhang, Y. (2021a). "A physical realization of porpoise biosonar concerning sound reception," *Appl. Phys. Lett.* **119**, 094103.
- Song, Z., Zhang, J., Ou, W., Zhang, C., Dong, L., Dong, J., Li, S., and Zhang, Y. (2021b). "Numerical-modeling-based investigation of sound transmission and reception in the short-finned pilot whale (*Globicephala macrorhynchus*)," *J. Acoust. Soc. Am.* **150**, 225–232.
- Song, Z., Zhang, Y., Mooney, T. A., Wang, X., Smith, A. B., and Xu, X. (2018). "Investigation on acoustic reception pathways in finless porpoise (*Neophocaena asiaorientalis sunameri*) with insight into an alternative pathway," *Bioinspir. Biomim.* **14**, 016004.
- Song, Z., Zhang, Y., Thornton, S. W., Li, S., and Dong, J. (2017). "The influence of air-filled structures on wave propagation and beam formation of a pygmy sperm whale (*Kogia breviceps*) in horizontal and vertical planes," *J. Acoust. Soc. Am.* **142**, 2443–2453.
- Varanasi, U., Feldman, H. R., and Malins, D. C. (1975). "Molecular basis for formation of lipid sound lens in echolocating cetaceans," *Nature* **255**, 340–343.
- Wei, C., Au, W. W. L., Song, Z., and Zhang, Y. (2016). "The role of various structures in the head on the formation of the biosonar beam of the baiji (*Lipotes vexillifer*)," *J. Acoust. Soc. Am.* **139**, 875–880.
- Wei, C., Houser, D., Erbe, C., Mátrai, E., Ketten, D. R., and Finneran, J. J. (2023). "Does rotation increase the acoustic field of view? Comparative models based on CT data of a live dolphin versus a dead dolphin," *Bioinspir. Biomim.* **18**, 035006.
- Wei, C., Song, Z., Au, W. W. L., Zhang, Y., and Wang, D. (2018). "A numerical evidence of biosonar beam formation of a neonate Yangtze finless porpoise (*Neophocaena asiaorientalis*)," *J. Theor. Comp. Acoust.* **26**, 1850009.
- Wei, C., Wang, Z., Song, Z., Wang, K., Wang, D., Au, W. W. L., and Zhang, Y. (2015). "Acoustic property reconstruction of a neonate Yangtze finless porpoise's (*Neophocaena asiaorientalis*) head based on CT imaging," *PLoS One* **10**, e0121442.
- Zhang, Y., Song, Z., Wang, X., Cao, W., and Au, W. W. L. (2017). "Directional acoustic wave manipulation by a porpoise via multiphase forehead structure," *Phys. Rev. Appl.* **8**, 064002.